Aerosols Impact on Optical Satellite Transmission

Amélie Gressier
École Nationale de l'Aviation Civile ENAC 31400 Toulouse France
Karine Caillault
Office Nationale d'Études et de Recherches Aérospatiales ONERA DOTA, Université Paris Saclay, F-91123 Palaiseau France

Optronics sensors, on board satellites are used for remote sensing and telecommunications but are submitted to meteorological conditions and among them cloud cover and aerosols. Aerosols presence in the field of view could be one of the key factor limiting performances of these sensors. The goal of this study is to predict optical transmission of a satellite's sensor due to aerosols with a Monte-Carlo method. Geometrical and optical properties required to build the model are obtained from Cloud–Aerosol Lidar with Orthogonal Polarization (CALIOP) measurements. Atmospheric scenes containing aerosols are generated and transmission spectra are obtained along the line of sight of a virtual satellite. To evaluate the impact of aerosols on the optical link, the probability of a transmission being greater than a threshold is calculated. Different areas are selected and relevant satellite's configurations are investigated: geostationary, low earth orbit, nadir view angle or tilted view. Results discussion points out the impact of climates and environments but also the importance of the satellite instrument's angle of view in the optical transmission between ground stations and satellites.

List of abbreviations

CAD	Cloud Aerosol Discrimination
CALIOP	Cloud-Aerosol Lidar with Orthogonal Polarization
CALIPSO	Cloud Aerosol Lidar and Infrared Pathfinder Satellite Observations
CNES	Centre National d'Etudes Spatiales
HDF	Hierarchical Data Format
HERA	Hybrid Extinction Retrieval Algorithms
LEO	Low Earth Orbit
LIDAR	Light Detection and Ranging
LOS	Line-of-Sight
NASA	National Aeronautics and Space Administration
RADAR	Radio Detection and Ranging
SCA	Scene Classification Algorithms
SYBIL	Selective Iterated BoundarY Locator

I. Introduction

Studying the availability of the optical-link between a satellite and the ground is becoming necessary to transfer data by selecting ground station localisations but also for defense activities and satellite sensors validations. The electro-optical performance of a satellite sensor used for remote sensing, or telecommunications can be strongly affected by meteorological conditions along its LOS. Clouds or aerosols can either produce an attenuation of the target signal or an increase in background radiation because of thermal emission or sunlight scattering. Cloud cover impact on the optical link has already been studied [1]. Aerosols have not been investigated yet and their effect on optical telecommunications are not well documented.

Ground lidars are efficient tools for getting information about optically thin particles but their results are restricted to a limited set of locations on the earth's surface. Remote sensing observations from satellites offer opportunities to provide an unprecedent aerosols survey on a global scale and to estimate optical transmissions statistics. Among these satellites, CALIPSO, a joint U.S. NASA and French CNES satellite mission, launched in April 2006, is dedicated to the study of aerosols and thin clouds (with a detection limit as low as 0.01 in terms of optical depth) [2]. The payload includes CALIOP, which delivers, for the first time on a global scale, multiyear measurements of vertical profiles of cloud and aerosol backscattering properties. Detection performances of a satellite sensor can vary widely as a function of local meteorology and viewing geometry, and thus transmission statistics only based on cloud cover might be restrictive. Consequently, there is a need to get transmission statistics with aerosols layers to determine their importance. The degree of atmosphere transparency for which a communication is supposed to be successful is given by an attenuation threshold: above this threshold, the atmosphere is considered to be clear enough to obtain good transmission performances.

The aim of this study is to determine transmission statistics all around the world for different detection scenarios: various LOS configurations are considered depending on the satellite altitude and viewing angle. Transmission statistics help us compute the probability of having an attenuation superior to a threshold and conclude on sensor's performances. Statistics are obtained with a model of the optical transmission. This Monte-carlo model enables us to create a LOS configuration, place aerosols layers in the scene and evaluate the optical transmission. Aerosols layers properties are chosen by random draws from a dataset previously built: the aerosols climatology. The latter provides information on geometrical and optical aerosols properties all over the world and it is created with CALIOP level 2 products. Every layer detected is classified depending on several parameters : altitude, width and extinction coefficient. An important part of this work consists in determining the classification used to rank aerosols layers by studying their distributions. First, we have to study aerosols repartition given by CALIOP products and define classes to rank layers and from which the climatology is built. Then, we generate an important number of atmospheric scenes using the Monte-Carlo method and compute transmission statistics for various LOS configurations. Comparing attenuation probabilities to a threshold will help us conclude on optical-link availability.

The paper follows these work steps starting with a bibliographic study on optical telecommunications and LIDAR remote sensing technique II. The building method of aerosol occurrence climatology obtained from CALIOP is explained in section III. Then, the climatoloy is compared to an other study [3] to qualitavely validate our result. The methodology used to calculate transmission probabilities is described in section IV, with the assumption of horizontally infinitely wide aerosol layer. Two main applications are considered: a geostationnary satellite configuration to highlight environmental and climatic transmission differences and a LEO satellite which illustrates the importance of viewing angle. Statistical transmissions obtained with the Monte-Carlo method are discussed in the last part of the article.

II. Optical Remote Sensing for atmosphere applications

II.1. Optical Transmission

Optical telecommunications use the 1.55μm wavelength because it is a transmission window. However, there is no aerosols optical database available at this wavelength and as a first step, we use 532nm CALIOP lidar data. A study will be conducted to transpose results from 532 nm to 1.55μm, but it is not in the scope of this paper.

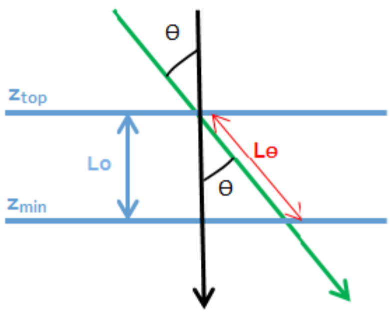

Figure 1. Oblique and vertical light beam geometry travels in an atmospheric layer.

The objective is to evaluate the transmission along the satellite's LOS. Optical attenuation, in decibel, is computed from the transmission T :

$$Attenuation = 10 \times logT \quad (1)$$

Transmission, in visible wavelength, is obtained by studying interactions between light and matter meaning diffusion and absorption. Transmission T is computed from optical depth τ :

$$T = e^{-\tau} \quad (2)$$

Aerosol layer optical depth corresponds to the integration along the LOS of the extinction profile which is the addition of light diffusion and absorption. It depends on the layer width and its radiative characteristics. If z_{top} is the top layer altitude, z_{min} the bottom layer altitude and k_{ext} the extinction coefficient, optical depth is defined as [4] :

$$\tau_{ext} = \int_{z_{min}}^{z_{top}} k_{ext}(z)\, dz. \quad (3)$$

Optical depth varies depending on the viewing angle : the more the angle is important, the longer the light beam path is. Light beam geometry is detailed on Figure 1. L_0 is the vertical light beam, L_θ is the distance travelled by an oblique light beam and θ is the viewing angle. The two blue lines represent the atmospheric layer. k_{ext} is the mean extinction coefficient for the aerosol layer. Optical depth for a vertical light beam (black arrow on Figure 1) is expressed as follows:

$$\tau_0 = k_{ext} \times L_0 \tag{4}$$

If the viewing angle is modified, the distance travelled in the layer increases (green arrow on Figure 1) and the optical depth is modified as:

$$\tau_\theta = \frac{k_{ext} \times L_0}{cos(\theta)} \tag{5}$$

Cosinus fonction decreases on the interval $\left[0; \frac{\pi}{2}\right]$ this is why for viewing angle from 0°to 90°, optical depth and light attenuation increase if we consider the extinction coefficient constant in the given layer.

II.2. Aerosol LIDAR Remote sensing

Aerosols are solide suspended particles in the low atmosphere. They include smoke, nitrates, sulphates and carbon components. 6000 megatonnes of aerosols are injected into the atmosphere every year. They come from natural sources like volcanic eruptions but also from human activities and biomass burning. Aerosols can be ranked into five classes: clean marine, desert dust, polluted continental, clean continental and stratopsheric [5]. In this study we focus on the tropospheric aerosols and we do not take into account layers detected above 10 km since stratospheric aerosols contribution is negligible. Remote sensing is widely use to characterize clouds, aerosols and atmospheric gases and requires a precise detector. LIDAR is an active remote sensing technique that emits a monochromatic light pulse. The light beam will interact with molecules along the LOS and will be attenuated by diffusion and absorption. The intensity of the back-scattered signal collected by the telescope depends on atmopsheric layers crossed by the beam. The LIDAR equation corrected from noise is as follows, with P the optical back-scattered power, A the surface receptor, r the distance between the receptor and the diffusive source, E_0 the laser power source, ξ the lidar parameter, β the back-scattering coefficient and T the transmission [6] :

$$P(r) = \frac{A}{r^2} \times E_0 \times \xi \times \beta(r) \times T^2 \tag{6}$$

Noise is supressed and the filtered signal is digitalized for computer processing. Compared to RADAR, LIDAR has an excellent directivity and is suitable for 3D scanning of structures like cloud, plume, whirlwind and aerosols. This technique is also different from infrared detection because it does not depend on temperature.

Satellite data used in the study are retrieved from CALIOP lidar instrument aboard CALIPSO satellite launched in 2006. The satellite is in a low earth orbit, at 705 km of altitude and revisit time is 16 days. The instrument emits two intense light pulses at 532nm and 1064nm. The visible wavelength is used in the present study because the other one is noisy and difficult to use. CALIOP provides different products for atmospheric studies and with different levels. Level 1 products are derived from level 0 raw products. They contain calibrated lidar profiles on a half satellite orbit. Several algorithms are applied to level 1 products to obtain level 2 [7]. The first step consists in detecting particles layers from backscattering coefficient profiles with SYBIL thresholding algorithm. When the attenuation is higher than in clear-sky condition a layer is defined. Once a layer is detected and spacially constrained, it is classified as cloud or aerosols by SCA algorithm based on optical and physical properties. Those properties are linked to the backscattered coefficient at 532nm, reflectance, temperature and pression. Finally, HERA algorithm provides the extinction coefficient which is necessary to compute transmission along the LOS [8]. We chose to work with level 2 layer products, with 60 m and 5 km vertical and horizontal resolutions.

II.3. Data Processing

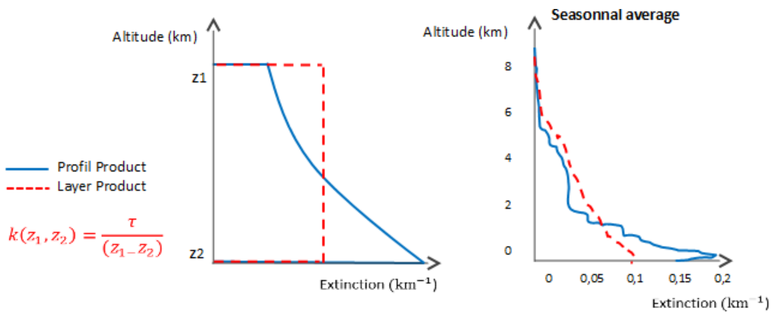

Figure 2. Schematic representation of profile product in blue and layer product in red for one layer (left). Schematic seasonnal average of the extinction coefficient over the Atlantic at night (right).

Detection algorithms provide two different types of products: layer and profile [8]. A Layer product is an integration of aerosols features detected in the atmosphere. Profile products provide parameters of interest for each altitude whereas layer products report properties by layer of particles detected. Differences between the two products is an important point in the data processing and interpretation. One HDF layer product file corresponds to 10 Mo whereas profile file weight 120 Mo in average. On the other hand, layer product degrades the extinction profile. The hypothesis of aerosols being uniformely distributed on a layer can be untrue. It may result in an underestimation of extinction at low altitudes and overestimation at high altitudes as shown in Figure 2 [9]. Average extinction coefficient is computed by dividing optical depth by geometrical width. For data storage and processing reasons, we chose to work with aerosols layer products. They directly provide layers top and bottom altitudes which makes it easier for data computing and modelling.

Each file contains features which are associated to a number of detected aerosols layers between 0 and 8. For each layer, latitude, longitude, top and bottom altitudes, optical depth, type of aerosols and flags are detailed [10]. Flags provide quality measurement information and help us sort layers. Each layer is filtered with the following items :

- **CAD Score** $[-100; 100]$ differenciates aerosol from cloud layer : negative values are set for aerosols. Only layer with a CAD score in $[-70; -100]$ are saved [11].
- **OD Uncertainty** is the uncertainty value on optical data. It is really difficult to obtain a good uncertainty so only values with a 99.9 flag are deleted.
- **Extinction Flag** indicates if detection algorithms converged. It is encoded in 16 bits.
- **Day Night Flag** provides information on measurement conditions: if the layer was detected at night or during the day.

III. 3D Aerosols Climatology Construction

The main goal of this section is to obtain global scale statistics on aerosols optical and geometrical parameters. Optical depth, top and bottom altitudes are retrieved from CALIOP's files and then, extinction coefficient and width are calculated. To obtain aerosols frequency distributions it is necessary to create classes of altitude, width and extinction coefficient. These uniform classes are used to rank detected layers and to model the atmosphere with random draws in the Monte-Carlo method. The classification is the first step to create an aerosol climatology. The latter is a long-time and global scale dataset that provides statistical information on geophysical parameters. In the present study the goal is to build a climatology on aerosols layers optical and geometrical properties. The grid used in the climatology has a 2.5°by 2.5°latidunal and longitudinal resolution in order to have a sufficient amount of data [12]. CALIOP's measurements from june 2006 to april 2018 are used to complete the climatology.

III.1. Aerosols distributions

We compute the number of classes for each parameter by studying aerosol frequency distributions. As an example, if all detected layers have a width of 2km only one class is defined for this parameter: $[0; 2]$. The study is conducted with products from the year 2010 and for the entire world but also for six zones (5°by 5°grid). Each spot is representative of a given environment (marine, continental, desert, tropical) whereas the global study is an average computed with all meshes. Grid location is detailed in Figure 3.

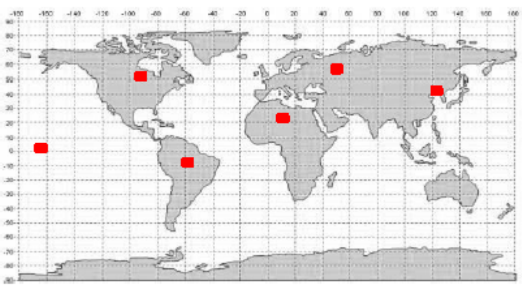

Figure 3. Localisation of the six 5°by 5°grid chosen for frequency distributions study.

Cumulative frequencies and histograms are plotted for each regional zone and on a global scale (Figure 4 and Figure 5). Aerosols distribution in altitude points out zonal differences : layers detected between $[0; 2]$km represent 20% of all layers for the desertic area compared to the oceanic one where there are predominant and represent 95% of the total. Continental areas are more or less similar : more than 50% of all the layers detected are located below 5km. In average, more than 60% of all layers are detected below 2km and layers located above 5km are a minority : 10% of the total (Figure 4a). Differences for the extinction coefficient are less striking. Aerosols layers have an extinction coefficient lower than

$0.25km^{-1}$: a minimum of 70% for the tropical area and a maximum of 95% for the Pacific Ocean. In average 90% of all the layers detected have an extinction coefficient below $0.25km^{-1}$ and less than 1% of the total have a $1km^{-1}$ extinction (Figure 4b). Layer width is the difference between top and bottom altitudes of each layer. 45% of layers detected above the Sahara desert have a geometrical width between 0 and 1km, 85% above the Pacific Ocean, 50% for the tropical area and 65% above Russia. In average 70% of all layers have a width between 0 and 1km, and 5% exceed 2km (Figure 4c).

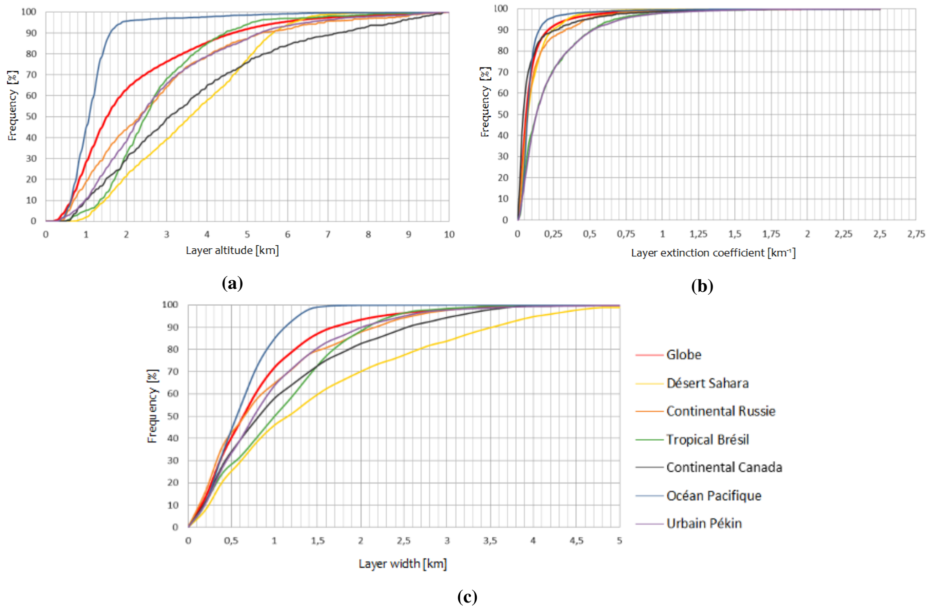

Figure 4. Aerosols cumulative frequency distributions in altitude (a), extinction coefficient (b), width (c) for a global average and six 5°by 5°areas representative of a given environment.

Frequency distributions highlight differences between continental and oceanic areas. It seems interesting to differenciate those two environments and create different classes. A new study is conducted with 15°by 15°meshes. Russia is chosen to represent continental area and the Pacific for oceanic regions. Indeed, Russia's distributions are close to the global average and Pacific is more reliable than Atlantic due to aerosols transport. Parameter's classes are defined for the global average as well. From cumulative frequencies, growth rate is computed in each point and tangents are plotted. Tangents intersections points are representative of slope changes. From slope changes and frequency histograms, uniform classes are defined. Figure 5 shows extinction coefficient histograms for oceanic area after the definition of classes. This method is applied to all parameters for continental, oceanic and global areas (Figure 4).

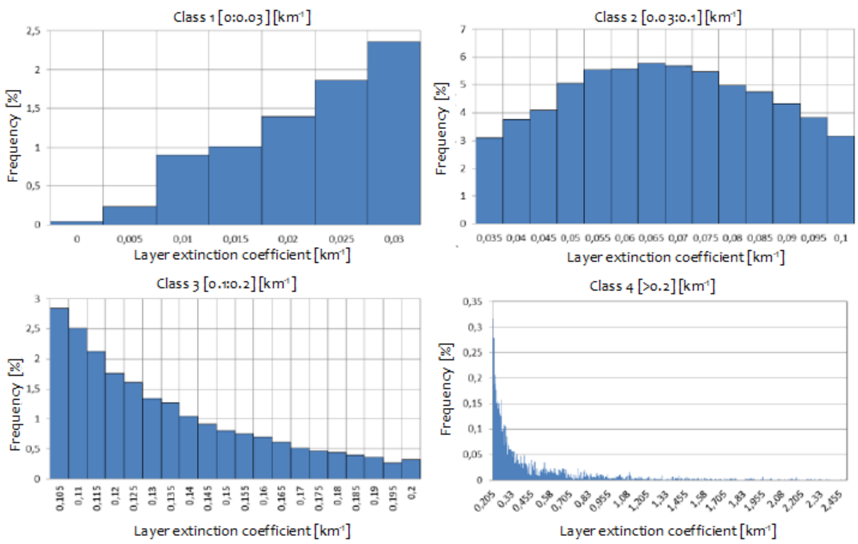

Figure 5. Extinction coefficient frequency histograms of Pacific ocean area and for the 4 classes defined. This study is derived from the 15°x15°grid data over the Pacific Ocean.

III.2. Probabilities calculation

As shown in section III.1 three different climatologies are built: one at a global scale, and the two others for continental and oceanic areas. The objective is to define joint probability density functions that describe aerosols layer occurency depending on three parameters : altitude, width and extinction coefficient. Joint probabilities are computed for all detected layers and differenciate night and day acquisitions. For the global scale climatology, aerosol layers are distributed into the following classes :

- Parameter x_1: top layer altitude. Depending on its value the layer is associated to the class: $[0; 2]$km; $[2; 5]$km or $[> 5]$km.
- Parameter x_2: layer extinction coefficient: $[0; 0.075]$km^1; $[0.075; 0.15]$km^{-1}; $[> 0.15]$km^{-1}.
- Parameter x_3: layer width: $[0; 1]$km; $[1; 2]$km; $[> 2]$km.

It leads to 27 combinations which means 27 possibilities to rank aerosols layers in the global scale climatology. In each 2.5°by 2.5°grid, we compute the probability of events combination P(x_1,x_2,x_3). It is the occurency of the combination (x_1,x_2,x_3) normalized by the number of layers detected by CALIOP N_T. The probability is then computed with [1] :

$$P(x_1, x_2, x_3) = \sum_{(x_1,x_2,x_3)} \frac{(x_1, x_2, x_3)}{N_T} \tag{7}$$

The same method is applied to the two others climatologies with different classes.

III.3. Results and comparison

From each mesh, various statistics can be calculated: occurrence of detected aerosols layers during the day or at night and for every season of the year, CALIOP's pass number and layer's detection probability... For every detected layer, the probability of events combination as described in Section III.2 is available. As an example, we want to retrieve the probability of detecting two layers over Paris during the day in summer, the first layer is located at 3km, has a width of 500m and an extinction coefficient of 0.06km^{-1}. The events are :

- x_1 belongs to the 2^{nd} class of altitude $[2; 5]$km.
- x_2 belongs to the 1^{st} class of extinction coefficient $[0.075; 0.15]$km^{-1}.
- x_3 belongs to the 1^{st} class of width $[0; 1]$km.

The class combination for the first layer over the two detected matches $[2; 1; 1]$. We have to look for the matrix collecting the data in summer, during the day, for the "first layer detected over two" and find the right cell fitting the latitude and longitude we are interested in.

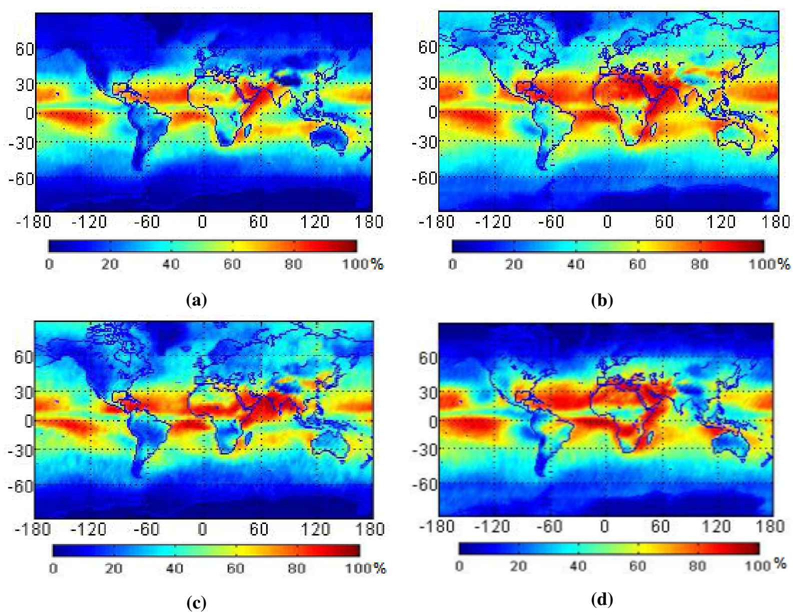

Figure 6. Occurency of at least one aerosols layer detected during the day (a), at night (b) for all seasons, in winter (c), during summer (d) whatever the time of detection.

Figure 6 illustrates the probability of having at least one aerosols layer for every grid during the day (Figure 6a) and at night (Figure 6b). At night the probability is higher because CALIOP LIDAR works at 532nm, in visible wavelength, and is limited by daylight. Thinnest layers are difficult to detect during the day. A large part of aerosols layers are detected at night above continents. Instument's performances seem better at night except off the Peru coast and the most important occurency appears in mid-latitudes. A lot of aerosols layers are detected in the inter-tropical convergence zone. Polar values are not reliable because snow limits instrument's performances. Figure 6 highlights seasonnal variations and the importance of this parameter in the climatology [13]. During summer (Figure 6c), an important part of aerosols layers are detected at mid-latitudes. At this moment of the year, aerosols are transported from the Sahara desert to the Atlantic Ocean and biomass burning are declared in South-America [14][15].

We compared our results with other studies [3][16] based on CALIOP's measurements in order to ensure our climatology. Winker's climatology [3] is built from 5 years of CALIOP level 2 profile products. The grid resolution is set to 5°by 5°and aerosols optical depth diurnal and seasonnal variations are studied. Data are filtered in a similar way: the CAD score between -20 and -100 and OD Uncertainty below 99.9. Figure 7 presents differences between Winker's study and our work. From statistical data, we plot daytime Figure 7b and nightime Figure 7d average aerosol optical depth and we compare them to Winker's results 7a and b. Geographical distribution is similar: the most important optical depth is found central Africa and south-east Asia. On the other hand, our climatology underestimates extinction coefficients and affects optical depth's computation. Profile products are averaged to obtain layer products (see Section II.3) which results in an extinction coefficient underestimation. Moreover, aerosols layers are mainly found below 2 km and these layers have the highest extinction coefficient. This issue could explain differences between Winker's optical depth values obtained from profile products and our results. Comparisons conducted in a desertic aera with a climatology built using layer products [16] show a good agreement with our results. It strenghtens the hypothesis of extinction's underestimation when using layers products.

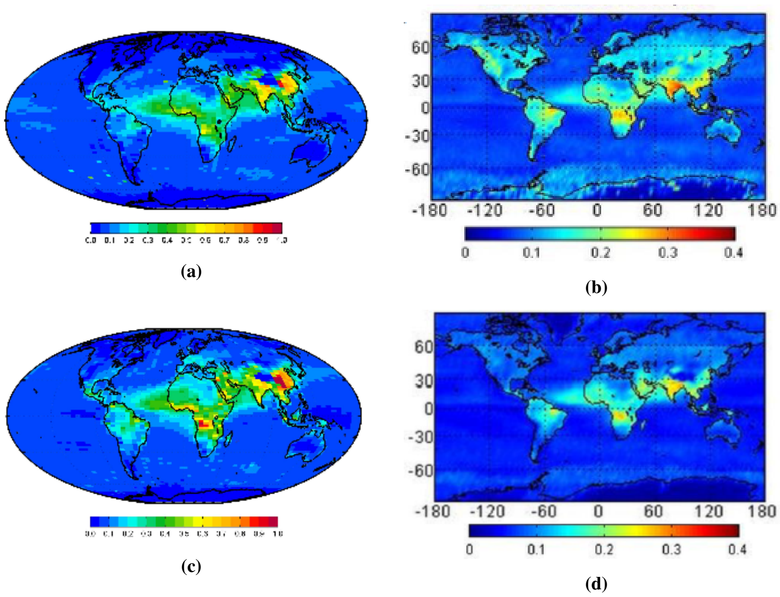

Figure 7. Average daytime(a) and nighttime (c) aerosol optical depth at 532 nm using January 2007 to December 2011 profile products from Winker's climatology. Average daytime(b) and nighttime (d) aerosol optical depth at 532 nm using June 2006 to April 2018 layer porducts from our climatology.

IV. Satellite sensor performance calculations and optical transmission results

The goal of this section is to compute LOS transmission from a geostationnary or a low-earth-orbiting satellite. Statiscal information is obtained from an important number of simulations.

IV.1. Viewing geometry and parameters

Satellite's position and instrument optical's LOS are defined with : latitude and longitude in degree, altitude in km, azimuth (angle between north and LOS) in degree and the viewing angle in degree. Either the satellite is geostationnary or LEO, its altitude is much higher than troposphere's altitude and first aerosols layers are found below 5km. But, for a same viewing angle the part of the atmosphere crossed by the LOS will be different depending on the satellite altitude. LOS's position in latitude and longitude is used to locate which part of the atmosphere is crossed in our climatology. It is calculated with 1km increment below 100km. Satellite's altitude is always above 100km but no aerosols layers are found above this altitude.

Viewing angle's range is different from a geostationnary and a LEO satellite. A geostationnary satellite covers a large part of the globe but observes the earth with a smaller range of viewing angle. The field of view is calculated with α defined as the angle between the vertical and Earth tangent :

$$\alpha = sin^{-1}(\frac{R_T}{R_T + h_{satellite}}) \tag{8}$$

For a geostationnary satellite (36000 km), 2α =17.4° so the viewing angle varies from -90° (vertical) to -75° and azimuth from 0 to 360°. For the LEO's case the satellite is placed at 700 km and 2α = 120°.

IV.2. Transmission calculation and Monte-Carlo algorithm

Atmospheric scenes are generated by a Monte Carlo method. This model enables us to build scenes containing rectangular finite aerosols layers, up to eight. Convergence is ensured thanks to a great number of generated scenes. Random draws are performed to get the aerosols layer's property values (altitude, width and extinction coefficient), which are constrained by joint probability densities calculated from aerosol occurrence climatology. Then, a sensor is placed in the scene with geometrical parameters described in IV.1.

Transmissions are then calculated for LOS crossing the scenes. Probability that a transmission T is greater than a given threshold T_t is given by the following equation where k stands for the number of scenes:

$$P(T \geq T_t) = \frac{\Sigma_k(T \geq T_t)}{\Sigma_k} \tag{9}$$

P(T$\geq T_t$) is equal to 1 when the condition is fulfilled, and 0 otherwise. Based on the aerosols layers' joint probability densities (Equation(7)) sensor performances expressed as transmission probabilities are determined. The impact of aerosols layers presence on optical-link is translated in terms of probabilities higher than a prescribed threshold P_T. This can be written as: $P(T \geq P_T)$.

IV.3. Geostationnary satellite's sensor performances

First, we test the geostationnary's configuration : the satellite is placed at 36000 km at 0°latitude and 0°longitude. Transmission probabilities are averaged over all the grid meshes of a zone defined in latitude and longitude. Every grid is considered with a different viewing angle. This study enables us to highlight environmental and seasonnal performances.

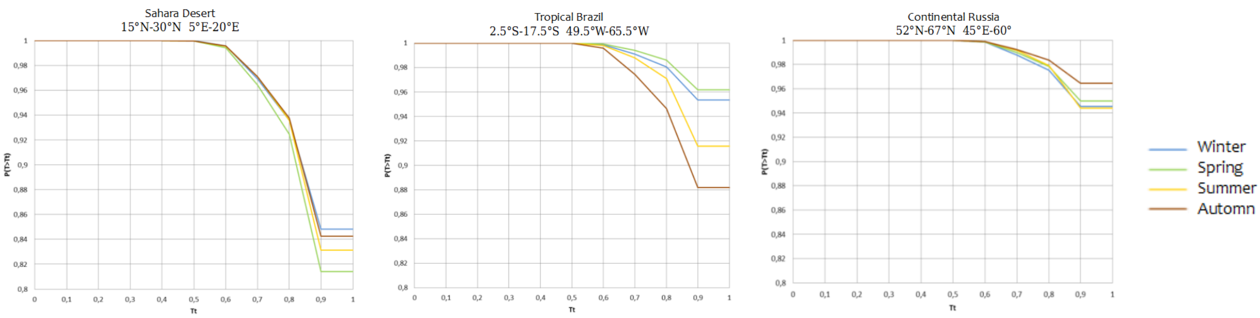

(a) (b) (c)

Figure 8. Transmission probabilities superior to a threshold for 15°x15°grid above Sahara Desert (a), Brazil (b) and Russia (c) for a geostationnary satellite's sensor (0°N and 0°E) operating during the day.

Figure 8 presents the probability of transmission being superior to a threshold for three 15°by 15° areas above the Sahara Desert (Figure 8a), Brazil (Figure 8b) and Russia (Figure 8c). The highest probability of transmission is found over Russia with $P(T = 1) \geq 0.94$ for all seasons. The desert area presents a probability $P(T = 1) \geq 0.85$ in winter. In all cases, $P(T = 1) \geq 0.5$, matching a -3 dB attenuation level, is respected. This value is often used in sensor's specifications for atmospheric attenuation. Seasonnal variations depend on the region observed. We note that during summer transmission probabilities are often low for all areas : $P(T = 1) = 0.830$ for the Sahara, $P(T = 1) = 0.915$ for Brazil and $P(T = 1) = 0.935$ for Russia. To explain those differences, seasonnal aerosol layers occurencies and optical depth are plotted (Figure 9) for the season showing the lowest transmission probability. There is more than 80% chance to find at least one aerosols layer above the Sahara desert (Figure 9a) and the average optical depth is 0.3 (Figure 9d) in spring. Aerosol optical depth reaches 0.4 in automn above Brazil (Figure 9e) and 0.15 in Russia during summer (Figure 9f). Considering only aerosols layers, continental areas at midlatitude present the highest transmission probability compared to desertic and tropical regions.

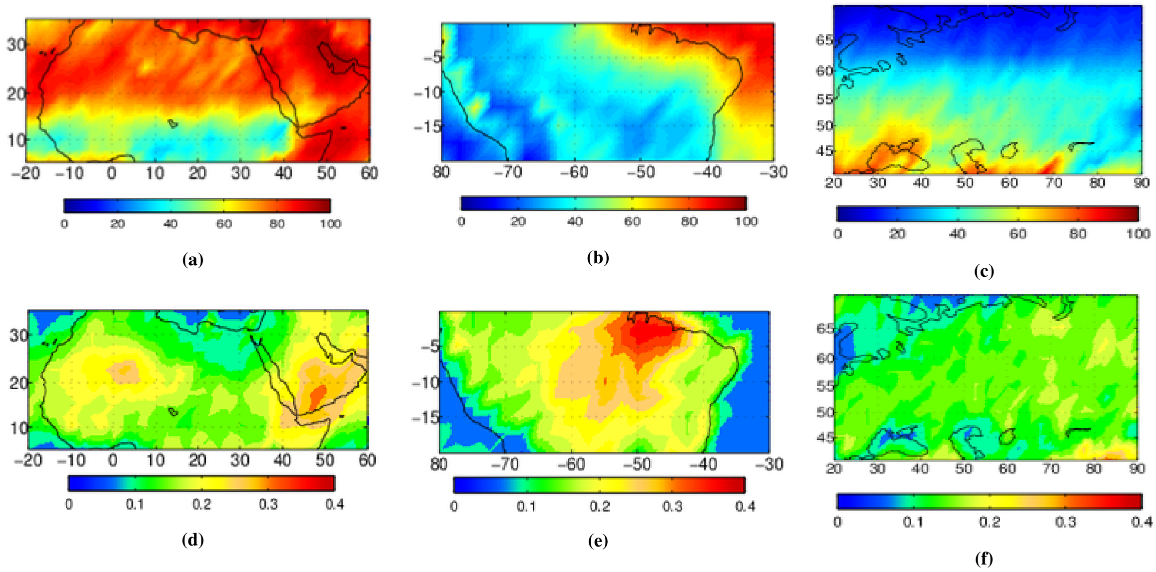

Figure 9. **Occurency of at least one aerosol layer detected during spring above the Sahara desert (a), during automn above Brazil (b) and during summer above Russia (c). Average aerosol optical depth during spring above the Sahara desert (d), during automn above Brazil (e) and during summer above Russia (f).**

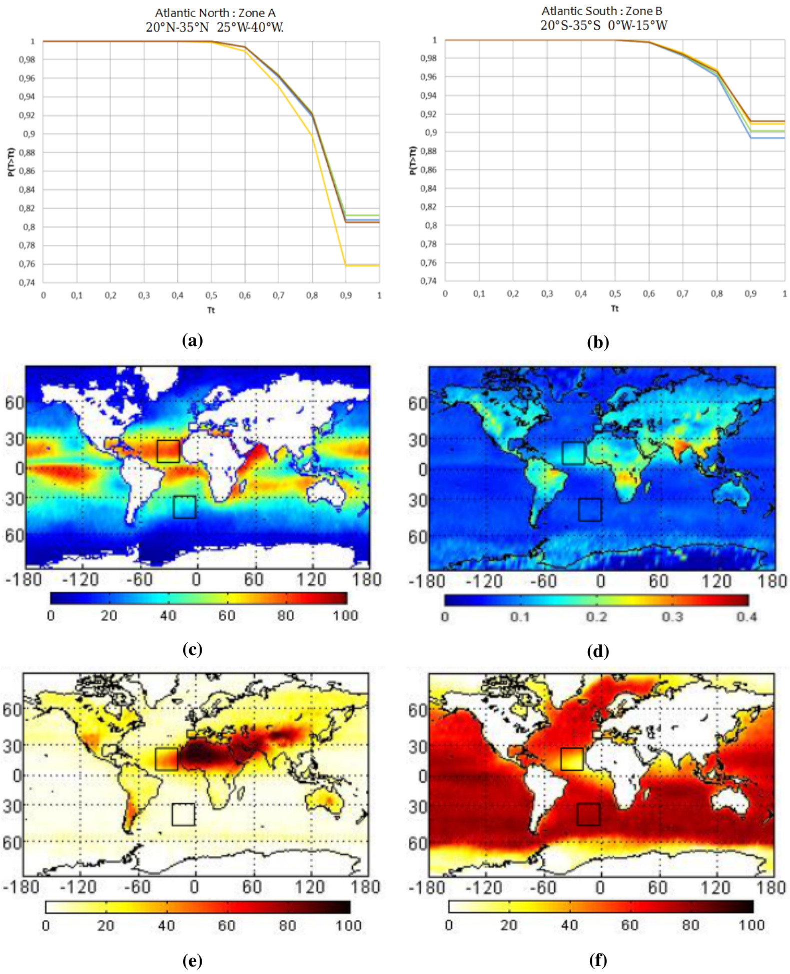

Figure 10. **Transmission probabilities superior to a threshold above two oceanic areas: zone A $[20^\circ N - 35^\circ N; 25^\circ W - 40^\circ W]$ (a) and zone B $[20^\circ S - 35^\circ S; 0^\circ W - 15^\circ]$ (b) for a geostationnary satellite's sensor operating during the day in winter (blue), spring (green), summer (yellow) and automn (brown). Occurency of at least one aerosol layer detected above oceans (c), average aerosol optical depth (d), occurency of at least one aerosol layer detected and classified as desert dust above oceans (e) and as clean marine (f) for all seasons. Black squares represent areas targetted for transmission probabilities.**

An oceanic climatology was built (see section III) and it seems interesting to study transmission probabilities from a geostationnary satellite sensor focusing on oceanic areas. Two regions are targetted : zone A $[20°N - 35°N; 25°W - 40°W]$ and zone B $[20°S - 35°S; 0°W - 15°]$ in the Atlantic Ocean. There are represented by black squares on Figure 10. The probability is higher in zone A : $P(T = 1) \leq 0.81$ than in zone B $P(T = 1) \geq 0.89$ (Figure 10a and b). The probability of detecting at least one aerosols layer is lower in the north (90 %) than in the south (10 %) (Figure 10c). Moreover, optical depth is higher in the nothern part of the Atlantic Ocean between 0.1 and 0.2 and below 0.1 in the southern part (Figure 10d). This could be explained by destertic aerosol transports from the Sahara to South America especially affecting the transmission in summer [17]. To comfort this hypothesis, we plot occurency of clean marine and desert dust aerosols retrieved from CALIOP lidar ratio (Figure 10 e and f). In the north, aerosols layers classified as clean marine are not as likely than desert dust aerosols.

IV.4. LEO satellite's sensor performances

Viewing angle has an impact on the LOS path (see Section II.1). LEO's configuration helps us point out transmission changes depending on the viewing angle. The satellite is placed at 700 km altitude in the middle of the targetted area, the Mediterranean region, and the viewing angle varies from -70°to -20°. This region is a good candidate to install ground stations. Seasonnal transmission probabilities are plotted for each viewing angle (Figure 11). The transmission's probability decreases when the viewing angle increases. This study indicates which angle to use in an optical-link communication for a ground station placed in the Mediterannean area. For a -5dB attenuation threshold, meaning a 0.3 minimum transmission, the viewing angle range is $[-90°; -30°]$. Below -30°, transmission's probability is not equal to 1 for all seasons (e). For a more restrictive threshold of -3dB, or a 0.5 minimum transmission, the viewing angle range is $[-90°; -60°]$ for $P(T > 0.5) = 1$ (Figure 11b).

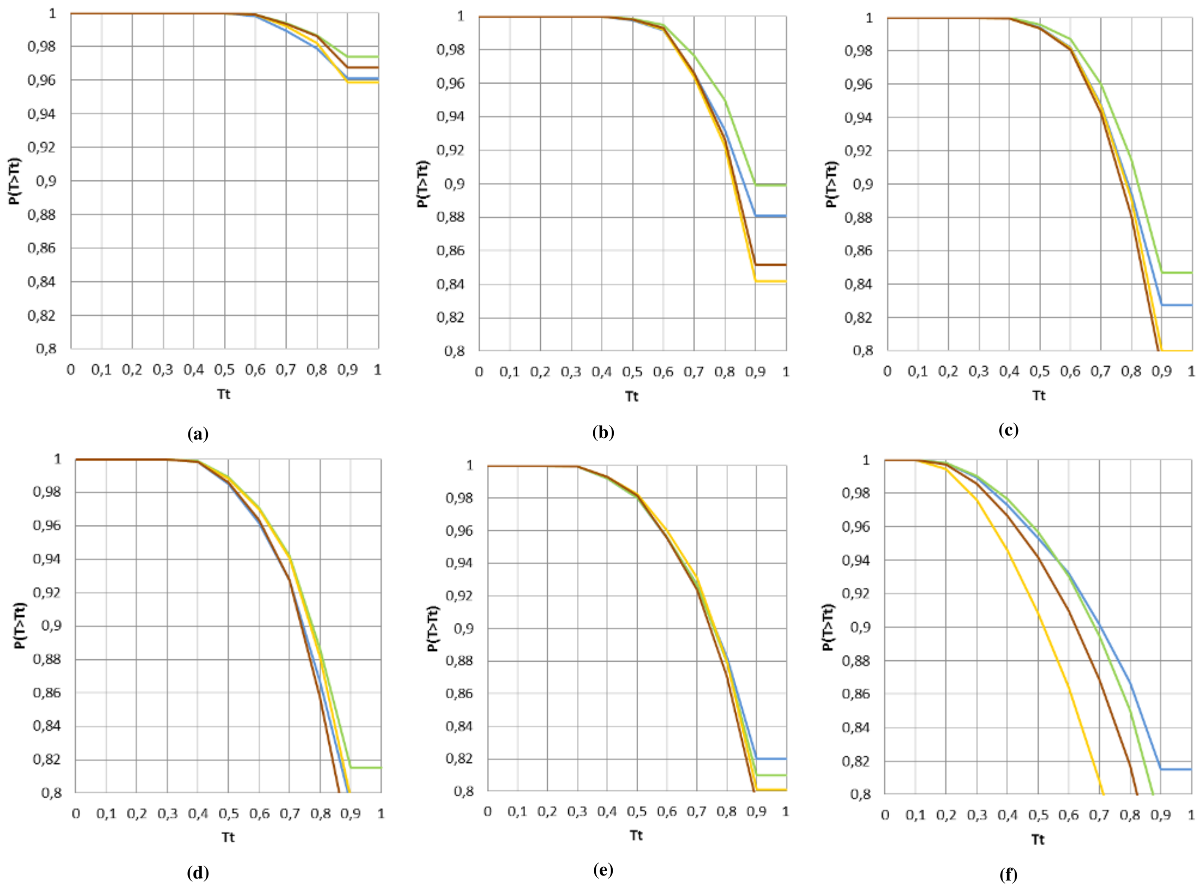

Figure 11. Transmission probabilities superior to a threshold for a LEO satellite's sensor placed at 37.5°N and 18°E operating during the day for a -70°(a), -60°(b), -50°(c), -40°(d), -30°(e), -20°(f), during winter (blue), spring (green), summer (yellow) and automn (brown).

V. Conclusion

To evaluate satellite's sensor performances, transmissions statistics along the sensor's LOS have been calculated based on a probabilistic approach. The impact of aerosol presence along the LOS was evaluated using an aerosol climatology built from CALIOP layer products. It is a new dataset that helped us improve our knowledge about aerosols geographical and optical properties and variability. It highlights important differences between oceanic and continental areas but also seasonnal and diurnal variations. The intertropical convergence zone is the place where there is the most important variation during the year. Different observation's configurations have been considered in order to demonstrate the potential of the proposed method for various applications. In particular, nadir-angle view allows a higher transmission probability and -3dB attenuation threshold is ensured. It has been shown in this work, that seasonal and geographical variations of aerosol occurrence affect sensor detection's performance. Transmission probability are strongly dependent on location: desertic or tropical areas show lower transmission levels and should be avoided in installing ground optical stations. They present an important probability of aerosols layers occurency and sometimes there are high in altitude. They also have optical properties able to limitate the transmission. Unpolluted continental regions should be prefered for station's installation.

We showed that layer products are likely to underestimate the extinction coefficient which could result in transmissions optimistic results. Optical depth is potentially higher for each layer detected which would affect the transmission. This issue could be resolved by using profile products even though they would require new ressources.

This study focused on aerosol impact on optical link. We pointed out that, alone, aerosols do not affect significantly the transmission but the Monte-Carlo model will have to be improved by adding clouds and atmopsheric gases to obtain more realistic transmission probabilities.

References

[1] A. Bizard, K. Caillault, C. Lavigne, A. Roblin, and P. Chervet. Application of cloud occurrence climatology from caliop to evaluate performances of airborne and satellite electro-optical sensors. *Journal of Atmospheric and Oceanic Technology*, 30, 2013.

[2] D. Winker, W. Hunt, and M. McGill. Initial performance assessment of caliop. *Geophysical Research Letter*, 34, 2007.

[3] D. Winker, J. Tackett, B.Getzewich, Z. Liu, M. Vaughan, and R. Rogers. The global 3-d distribution of tropospheric aerosols as characterized by caliop. *Journal of Atmopsheric Chemistry and Physics*, 13, 2013.

[4] A. Bizard. Climatologie des nuages haute altitude à partir du lidar caliop. Master's thesis, Université Montaigne Bordeaux 3, 2011.

[5] S. Jacquemoud. Fonctionnement du sytème atmosphérique, transfert radiatif et bilan énergétique de l'atmosphère. *Master Lecture*, 2016.

[6] R. Collis and P. Russel. *Laser monitoring of the atmosphere*. Springer-Verlag, Berlin, 1976.

[7] M.Vaughan, M. Pitts, C. Trepte, and D. Winker. *Data Management System - release4.10 Document*. No: PC-SCI-503 5.

[8] D. Winker, M. Vaughan, A. Omar, Y. Hu, K. Powell, Z. Liu, W. Hunt, and S. Young. Overview of the calipso mission and caliop data processing algorithms. *Journal of Atmospheric and Oceanic Technology*, 26, 2009.

[9] J. Tackett, D. Winker, B. Getzewhich, M. Vaughan, S. Young, and J. Kar. Calipso lidar level 3 aerosol profile product: version 3 algorithm design. *Journal of Atmospheric and Measurement Technique*, 11, 2018.

[10] M. Vaughan, K. Powell, D. Winker, and C. Hostetler. Fully automated detection of cloud and aerosol layers in the calipso lidar measurements. *Journal of Atmospheric and Oceanic Technology*, 26, 2009.

[11] CloudSat Science Team Meeting. *Cloud Aerosol Discrimination (CAD) in CALIOP version 4 level 2 data – CAD everywhere!*, 2016. Newport News, VA.

[12] M. Petitjean. Performances statistiques d'un capteur satellitaire en présence de nuages. Technical report, ONERA, 2016.

[13] D. Winker, J. Pelon, J. Coakley, J. Ackermann, R. Charlson, P. Colarco, P. Flamant, Q. Flu, R. Hoff, C. Kittaka, T. Kubar, H. Le Treut, M. McCormick, G. Megie, L. Poole, K. Powell, C. Trepte, M. Vaughan, and B. Wieckli. The calipso mission a global 3d view of aerosols and clouds. *American Meteorological Society BAMS*, 2010.

[14] D. Bou Karam. *Mécanismes de soulèvement des aérosols désertiques en l'Afrique de l'Ouest*. PhD thesis, Université Paris VI Sciences de l'Environnement, 2008.

[15] X. Ma, K. Bartlett, K. Harmon, and F. Yu. Comparison of aod between calipso and modis: significant differences over major dust and biomass burning regions. *Journal of Atmospheric and Measurement Technique*, 6, 2013.

[16] EGU General Assembly. *Dust aerosol optical depth above Sahara and Arabian Peninsula from CALIOP: comparison with MODIS Deep Blue and MISR*. Austria Copernicus MACC II Project, 2013.

[17] J.P. Vernier. *Les aérosols et le transport dans la haute troposphère et la stratosphère tropicale à partir des mesures du lidar spatial CALIPSO*. PhD thesis, Université de Versailles Saint-Quentin en Yvelines, 2012.